

See discussions, stats, and author profiles for this publication at: <https://www.researchgate.net/publication/50818571>

Vibronic structure in triatomic molecules : The hydrocarbon flame bands of the formyl radical (HCO). A theoretical study

ARTICLE *in* THE JOURNAL OF CHEMICAL PHYSICS · MAY 1998

Impact Factor: 2.95 · DOI: 10.1063/1.476138 · Source: OAI

CITATIONS

38

READS

22

3 AUTHORS, INCLUDING:



Per-Åke Malmqvist

Lund University

77 PUBLICATIONS 9,814 CITATIONS

SEE PROFILE

Vibronic structure in triatomic molecules: The hydrocarbon flame bands of the formyl radical (HCO). A theoretical study

Luis Serrano-Andrés,^{a)} Niclas Forsberg, and Per-Åke Malmqvist

Department of Theoretical Chemistry, University of Lund, Chemical Centre, P.O.B. 124, S-221 00 Lund, Sweden

(Received 10 July 1997; accepted 23 January 1998)

A theoretical study of the vibrational structure of the \tilde{X}^2A' ground and \tilde{B}^2A' excited states of the formyl radical, HCO, and its deuterated form, DCO, has been performed. The potential energy surfaces have been computed by means of a multiconfigurational perturbative method, CASPT2. The computed geometries and the harmonic and anharmonic frequencies are successfully compared to the available experimental information. The vibrational intensities of the transition $\tilde{B}^2A' \leftrightarrow \tilde{X}^2A'$ have been computed both for absorption and emission. The results lead to accurate determinations of several structural parameters and some reassignments of the vibrational transitions of the so-called hydrocarbon flame bands of the formyl radical. © 1998 American Institute of Physics. [S0021-9606(98)01916-3]

I. INTRODUCTION

The calculation by pure *ab initio* methods of the vibrational spectrum of a polyatomic molecule is a formidable task, even when the theoretical study is restricted to the harmonic approximation. For triatomic systems it is possible to fully compute and fit a global potential energy surface and use it to perform the vibrational analysis, including the anharmonicity corrections necessary to explore the dissociation limits. In the present study we have computed the potential energy surfaces of the ground, \tilde{X}^2A' , and excited state, \tilde{B}^2A' , of the formyl radical system, HCO, by means of the complete active space self-consistent field (CASSCF) method and a multiconfigurational perturbative method, CASPT2. The computed surfaces have been fitted to fourth-order force fields and the harmonic and anharmonic vibrational frequencies have been obtained by standard perturbation theory. In addition, the Franck-Condon factors for the absorption and emission processes involving the mentioned states have been computed using a new and efficient procedure in which recursion formulae are employed to compute the overlap integrals of two sets of multidimensional harmonic oscillators. Intensity borrowing effects are computed by including the dependence of the electronic transition moments on the nuclear coordinates formulated in terms of oscillator ladder operators.

The HCO radical is an intermediate in thermal and photochemical processes important in combustion, atmospheric, and interstellar chemistry, especially as a source of atomic hydrogen through its unimolecular dissociation on the ground-state potential surface.¹ A large number of experimental and theoretical studies have been focused on this system. Microwave² and infrared^{3,4} spectroscopy were used to obtain the geometries and frequencies of the ground state. The first spectrum arising by an electronic transition in HCO

was obtained in absorption for the so-called red band system, between 860–460 nm.⁵ That and subsequent studies^{6–11} determined the presence of the \tilde{A}^2A'' state correlating, together with the ground state, to the $1^2\Pi$ electronic state at the linear nuclear geometry, their splitting being a consequence of the Renner-Teller effect. In the energy range 410–230 nm the so-called hydrocarbon flame bands appear. They were observed in 1934 and assigned to HCO by Vaidya.^{12–14} The first complete electronic, vibrational, and rotational analysis was performed by Dixon in 1969.^{15,16} The absorption counterpart of the hydrocarbon flame bands was observed by Milligan and Jacox^{17,18} and assigned to the $\tilde{B}^2A' \leftarrow \tilde{X}^2A'$ and $\tilde{C}^2A'' \leftarrow \tilde{X}^2A'$ systems. The bound and resonance states of the molecule, especially the ground state and the \tilde{B}^2A' excited state, have been extensively studied using laser-induced fluorescence,^{19,20} resonance two-photon ionization,²¹ fluorescence excitation,^{22,23} stimulated emission pumping,^{22,24} and disperse fluorescence²⁴ spectroscopy in gas phase and jet-cooled HCO. The equilibrium CO bond distance in the \tilde{B}^2A' and \tilde{C}^2A'' excited states was found to be larger and the bond angle smaller than in the ground state. This gives rise to two progressions in both the bending and the CO stretching modes. Despite the extensive investigations, issues such as the assignment of the proper bending and stretching frequencies in the \tilde{B}^2A' state or the presence of bands belonging to the \tilde{C}^2A'' state at low energies are still under controversy (see discussion in Ref. 22).

A number of theoretical studies have helped to understand the experiments. Since the early work by Walsh,²⁵ that correctly predicted the electronic configuration and the bent structure of the ground state, the most extensive set of studies on the different electronic states of the system has been carried out by Peyerimhoff and co-workers.^{26–31} Other initial *ab initio* studies used small basis and CI spaces.^{32,33} Calculations on molecular potential energy hypersurfaces have also been performed. The first realistic surface for the ground state was obtained by Bowman *et al.*³⁴ at the SDCl+Q level

^{a)}Present address: Departamento de Química Física, Universitat de València, Dr. Moliner 50, Burjassot, E-46100 Valencia, Spain.

using more than 2000 geometries. The empirically corrected *ab initio* surface has been employed for different time-independent and time-dependent dynamical calculations^{35–37} obtaining qualitatively correct results. Recently, a more accurate and fully *ab initio* ground state surface has been obtained by means of the CASSCF/ICCI+Q method and large basis sets.³⁸ To our knowledge no equivalent studies have been performed on the excited states surfaces, except for the recent study on the \tilde{A}^2A'' state.³⁹ Geometries, energies, and harmonic frequencies have however been reported.^{40,41}

II. METHODS

A. *Ab initio* calculations of the potential energy surfaces

The CASSCF method and multiconfigurational second-order perturbation theory, CASPT2, were used to compute the electronic potential energy surfaces in the formyl radical system. Energies were computed at the CASPT2 level while the remaining parameters have been calculated at the CASSCF level. The CASPT2 method^{42–44} calculates the first-order wave function and the second-order energy with a CASSCF wave function constituting the reference function.⁴⁵ Recently, a level shift technique has been introduced,^{42,46} the so-called LS-CASPT2 approach, which can eliminate the effect of weak intruder states common in many calculations on excited states. After careful testing of different values of the level shift parameter, a value of 0.25 a.u. has been used in all the states. The CAS state interaction method (CASSI) was used to compute transition properties⁴⁷ at the CASSCF level. Intensities (oscillator strengths) were obtained by combining the CASSCF transition moments with CASPT2 evaluated excitation energies, a method which in a number of previous applications has proven to give accurate results.^{42,48}

The selection of the proper active space is the crucial step in the CASSCF/CASPT2 approach. In general, the active space should include all orbitals with occupation numbers appreciably different from two or zero in any of the excited states under consideration. This means that all near-degeneracy effects are included in the CASSCF reference function, and consequently there will be no large terms in the perturbation expansion. The ground state of the HCO radical has an electronic structure which might be described as follows (C_s symmetry):

$$(1a')^2_{O1s}(2a')^2_{C1s}(3a')^2_{O2s}(4a')^2_{CO\sigma}(5a')^2_{CH}(6a')^2_{O2p}(1a'')^2_{CO}(7a')^1_{C2p}.$$

The subindex corresponds to the predominant character of the orbital. The valence active space is completed by the $(2a'')^0_{CO*}$, $(8a')^0_{CO*}$, and $(9a')^0_{O3p}$ orbitals. When high accuracy is desired there are small effects regarding the selection of the active space to take into account. Some preliminary studies have to be performed to obtain a proper selection. The $1a'$ and $2a'$ core orbitals will be kept inactive together with the $3a'$ orbital (mainly composed by the $2s$ orbital of the oxygen) because they have occupations close to two in all the studied states. Calculations on the ground state using the valence active space, inactive (3,0), active (6,2), with the labels in parentheses representing the number of a'

and a'' orbitals, respectively, where the $8a'$ and $9a'$ orbitals were the correlating orbitals for the $CO\sigma$ bond and the O_{2p} lone pair. The $7a'$ orbital is singly occupied in the ground state. It is essentially the in-plane carbon $2p$ orbital, including important CO bonding character. The \tilde{B}^2A' state can be approximately described as obtained from the ground state by promoting one electron from the $6a'$ to the $7a'$ orbital. The former becomes a singly and the latter a doubly occupied orbital. In this case the correlating orbitals within the active space in the a' symmetry were mainly the antibonding $CO\sigma$ and $C_{3p,CH*}$ orbitals. In order to have a consistent active space for both states we included a new orbital of a' symmetry, leading to an active space (7,2) with nine active electrons. In this way, the character of the orbitals in the active space is therefore the same in both states. In practice it turned out that even for the proper description of the ground state vibrational frequencies it was important to have an orbital correlating the doubly occupied CH bonding orbital. The states have been computed as the first and second roots, respectively, of $^2A'$ symmetry in separate state-specific CASSCF calculations.

For the vertical calculations at the ground state equilibrium geometry we wanted to study a larger number of both valence and Rydberg states. In this case we use the valence active space plus three orbitals of a' symmetry and one orbital of a'' symmetry, corresponding to the $3s$, $3p$ low-lying Rydberg orbitals. This active space, used exclusively in the vertical calculations of Sec. III A, is therefore labeled (9,3).

To calculate the potential energy surfaces in the ground and \tilde{B}^2A' excited states we used atomic natural orbital (ANO) type basis sets⁴⁹ contracted to $[4s3p2d1f]$ for carbon and oxygen and $[3s2p1d]$ for hydrogen. For the vertical calculations at the ground state geometry these basis sets were supplemented with a $[1s1p1d]$ set of Rydberg type functions. The latter were determined following the procedure described earlier⁴⁸ and placed at the charge centroid of the $^1A'$ HCO cation.

The potential energy surfaces were computed on a three-dimensional grid around the CASSCF minima of both ground and excited states. Six different values for the CH length and five different values for the CO length and HCO bond angle were employed, using an interval of 0.025 bohr and 2.5 deg, respectively. Additionally, several geometries computed for larger values of the CH length coordinate have been included to account for the large anharmonicity effects related to that coordinate. A total number of 171 nuclear geometries were used for each of the two computed states. In addition to the energies, the transition dipole moments have been computed at all the geometries.

The vibrational modes are numbered following Mulliken's convention⁵⁰ in order of decreasing frequency within each symmetry species. Vibrational modes of similar character for different electronic states may then be numbered differently, and comparison to other studies should be made with caution.

The calculations have been performed with the MOLCAS-3 (Ref. 51) program package on IBM RS/6000 workstations.

B. Analytical representation and vibrational calculations

The chosen grid was considered to be adequate for fitting potential surfaces of local validity in the potential wells around the \tilde{X} and \tilde{B} minima. Basically, a third-degree polynomial in the internal stretch and bend coordinates was used. However, fourth-order terms were added for the CO distance and for the bending angle. The resulting 22-term polynomial is still much too inflexible to give a good surface, if the basic variables are chosen to be the bond distances and bending angle directly. We used exponential functions of the distances as bond stretch variables, and as bending variable the cosine of the angle, i.e.,

$$V(r_1, r_2, \theta) = \sum_{k=1}^{22} C_k x_1^{a_k} x_2^{b_k} x_3^{c_k},$$

$$x_1 = 1 - \exp(-\alpha_1(r_1 - r_{1e})),$$

$$x_2 = 1 - \exp(-\alpha_2(r_2 - r_{2e})),$$

$$x_3 = \cos(\theta_e) - \cos(\theta),$$

where suitable values of α_1 and α_2 were determined by some early experiments and then kept fixed. The above formulas also contain the initially unknown equilibrium distances. However, changes in these values are equivalent to mere scaling and translation of the basic variables, which does not affect the fitted function. The root-mean-square deviation of the fitted function from the computed energies was approximately 10^{-5} a.u. for both states.

The vibrational spectrum (for a nonrotating molecule) was computed in two different ways. Initially, the standard harmonic approximation expressions, including the effect of the anharmonicities, were employed.⁵² In addition, the vibrational spectrum was obtained by a variational solution of the $J=0$ Schrödinger equation using a basis set consisting of the joint set of harmonic oscillator (HO) wave functions for the two states. The basis sets comprised all HO states with a quantum number sum up to a certain limit. The variationally computed energies agree with the perturbation formula for the lowest states with a precision that first increases with larger basis sets. However, when the basis set is increased further, we observe a deterioration of the results, which we ascribe to the failure of accounting properly for linear structures. We will use the more accurate variational procedure to account for the low-energy spectrum for the absorption to the \tilde{B}^2A' state, while the harmonic approximation will be used in the remaining situations.

The lowest derivatives, up to fourth order, of the fitted potential functions were computed at the minima. Most of the fourth derivatives are not individually optimized but are determined, due to the nonlinear transformation described above, by the lower derivatives. Nevertheless, the accuracy of the fit gives some confidence that the quartic expansion can be used for the vibrational analysis.

In the vibrational analysis, the standard internal coordinates—the change from equilibrium in bond lengths and angle—were used. The dimensionless normal coordinates that enter the analysis are thus, for each state, a fixed

linear combination of such internal coordinates. The linear combinations are determined from a conventional harmonic vibrational analysis, closely following the so-called GF method of Wilson *et al.*⁵³ However, the coordinates are curvilinear, i.e., the mass tensor is not constant, so for the anharmonicity we did not want to use the standard formulas,⁵² which assume coordinates that depend linearly on the Eckart-frame cartesian coordinates. Corresponding formulae were derived, which also include the derivatives of the mass tensor due to nonlinearities. We found, however, that the additional terms, in the present case, were very small and could just as well have been neglected.

C. Vibrational intensities

Functions of the same type as those used for the potentials were fitted to the dipole moment and to the transition dipole moment components, μ_y and μ_z , for $\tilde{B} \leftarrow \tilde{X}$. Strictly speaking, the angular variable should now have been $\sin \theta$ rather than $\cos \theta$ for the z component (The internal frame is oriented with the y axis in the direction of the CO bond, and the z axis is perpendicular to it, with CH in the third quadrant of the yz plane.) The fit is good, however, (rms error = 10^{-3}) and since only angles considerably smaller than 180° are of interest in this study, we have simplified the procedure by using the same set of functions for all the properties studied.

Approximate spectra were computed with a very simple model. Harmonic oscillator wave functions were used as approximate vibrational wave functions. Oscillator strengths were then computed as

$$f = \frac{2}{3} \Delta E (\langle \chi_f | \mu_y | \chi_i \rangle^2 + \langle \chi_f | \mu_z | \chi_i \rangle^2),$$

where χ_f and χ_i are final and initial vibrational wave functions, and μ_y and μ_z are the transition moments. These are functions of the internal coordinates, and the brackets denote integration over these coordinates. Use of harmonic wave functions is such a crude approximation that only two types of approximate treatments of the integrals are worthwhile; treating the transition moment functions in the integrands as constants, or as linearly varying functions. The first choice immediately gives

$$f = \frac{2}{3} \Delta E (\mu_y^2 + \mu_z^2) S_{fi}^2,$$

which is the Franck–Condon approximation where the Franck–Condon factor S_{fi} is an overlap matrix element. The second choice, frequently called the “double harmonic” approximation, can be computed similarly, since the linear dependence can be expressed in terms of oscillator ladder operators which create or annihilate a single quantum. The result can therefore be expressed in terms of Franck–Condon factors S_{jj} involving intermediate states j that differ from i by at most a single excitation.

The Franck–Condon factors used in this study involve only displaced harmonic oscillators with three variables and fairly low quantum numbers. These can be computed by a number of well-known methods. However, in this case they were obtained by a program using a new algorithm.⁵⁴ One feature of this method is that the overlap matrix, which con-

TABLE I. Qualitative description of the electronic valence states of the CO and HCO systems using their main electronic configurations.

Linear ^a		Bent ^{b,c}
HCO $^2\Sigma^+$	CO $X\ ^1\Sigma^+$ $(1\pi)_{CO,2p}^4 (5\sigma)_{CH}^2 (6\sigma)_{CH}^1$	$(5a')_{CH}^2 (1a'')_{CO}^2 (6a')_{O2p}^2 (7a')_{CH}^1$
	HCO $^2A'$	
HCO $^2\Pi$	CO $a\ ^3\Pi$ $(1\pi)_{CO,2p}^4 (5\sigma)_{C2s}^1 (2\pi)_{CO^*,C2p}^1$	$(5a')_{CH}^2 (1a'')_{CO}^2 (6a')_{O2p}^2 (7a')_{C2p}^1$
	HCO $X\ ^2A'$	
HCO	HCO $A\ ^2A''$	$(5a')_{CH}^2 (1a'')_{CO}^2 (6a')_{O2p}^2 (2a'')_{CO^*}^1$
	CO $\pi \rightarrow \pi^*$ $(1\pi)_{CO,2p}^3 (5\sigma)_{C2s}^2 (2\pi)_{CO^*,C2p}^1$	
	HCO $B\ ^2A'$	$(5a')_{CH}^2 (1a'')_{CO}^2 (6a')_{O2p}^1 (7a')_{C2p}^2$
	HCO $C\ ^2A''$	$(5a')_{CH}^2 (1a'')_{CO}^2 (6a')_{O2p}^2 (7a')_{C2p}^2$
	HCO $^2A'$	$(5a')_{CH}^2 (1a'')_{CO}^2 (6a')_{O2p}^1 (7a')_{C2p}^2 (2a'')_{CO^*}^1$
	HCO $^2A'$	$(5a')_{CH}^2 (1a'')_{CO}^1 (6a')_{O2p}^2 (7a')_{C2p}^1 (2a'')_{CO^*}^1$

^aThe leading $(1\sigma)^2(2\sigma)^2(3\sigma)^2(4\sigma)^2\dots$ are omitted.^bThe leading $(1a')^2(2a')^2(3a')^2(4a')^2\dots$ are omitted.^cOrbitals called O $2p$ and C $2p$ actually have strong contributions from C $2p$ and O $2p$, respectively. O $2p$ is CO bonding, and C $2p$ is CO antibonding.

tains the Franck–Condon factors, is obtained as the product of a lower-triangular and an upper-triangular matrix, $\mathbf{S}=\mathbf{L}\mathbf{U}$, and similarly for other properties, the matrix elements are obtained as the product $\mathbf{L}\mathbf{X}\mathbf{U}$, where \mathbf{X} is the matrix elements of some property X computed over one single, centrally placed set of harmonic oscillator wave functions. The significance is that this formula is exact if the “central” matrix elements are exactly given. This implies that, to obtain the highest accuracy, the constant and/or higher order derivatives of μ_y and μ_z should be evaluated at the equilibrium geometry of this midpoint oscillator. The final results presented here for the vibrational intensities include derivatives up to fourth order of the electronic transition moment in the expression for the vibronic transition moments. The higher order terms, however, turned out to be of minor importance in the calculation of the intensities.

As previously explained, the variational method to compute the vibrational spectrum is used to describe the low-energy spectrum of the absorption to the HCO $\tilde{B}\ ^2A'$ state. The use of this approach seems important in a case like HCO where the CH stretch mode has large anharmonic corrections. The initial experiments showed that bands belonging to progressions in the first mode in the $\tilde{B}\ ^2A'$ state of HCO were visible in the spectrum only when the variational approach was used.

The theoretical spectra computed in the present study were convoluted with a Lorentzian function of full width at half maximum,⁵⁵ $\Gamma=h/(4\pi T_2)$, corresponding to a fictitious lifetime $T_2=130$ fs, to account for the finite experimental resolution and for the degrees of freedom, e.g., rotation, not considered here.

III. RESULTS AND DISCUSSION

A. The spectrum of the formyl radical

The formyl radical is formed by photolysis of acetaldehyde in a highly vibrationally excited triplet state.⁵⁶ The electronic structure of the low-lying states of HCO can however be better understood starting from the electronic structure of the CO molecule.³² The ground state of CO, $^1\Sigma^+$ essentially has the configuration $[\text{core}](3\sigma)^2(4\sigma)^2(1\pi)^4$

$(5\sigma)^2$, with the 5σ orbital as a carbon lone pair. Approaching the hydrogen atom along a linear path to the carbon results in the $^2\Sigma^+$ state of HCO. The 5σ orbital becomes the CH bonding orbital and the singly occupied 6σ orbital becomes the CH antibonding orbital. Another close state can be formed starting from the first excited state in CO, the $a\ ^3\Pi$ state, with the configuration $[\text{core}](3\sigma)^2(4\sigma)^2(1\pi)^4(5\sigma)^1(2\pi)^1$. The approach of the hydrogen in the same way as before leads to a state with a doubly occupied 5σ orbital, the $^2\Pi$ state of HCO. In this state the CH bond is stronger because of the addition of one electron to the CH bonding orbital. Due to the Renner–Teller effect the $^2\Pi$ state in linear HCO will split into two states along the bending coordinate. Following Walsh’s rules the π orbitals will also split into one strongly stabilized a' orbital and one a'' orbital.³² As was shown by calculations²⁶ a long time ago, the $^2\Pi$ state becomes lower in energy than the $^2\Sigma^+$ state, and therefore the states resulting from the Renner–Teller splitting are the $\tilde{X}\ ^2A'$ ground state and the first excited $\tilde{A}\ ^2A''$ state. The $^2\Sigma^+$ state has higher energy and it is strongly destabilized by the bending.²⁹

Table I describes the excited states of HCO that result from the $\pi \rightarrow \pi^*$ excited states of CO with electronic configuration, $[\text{core}](3\sigma)^2(4\sigma)^2(1\pi)^3(5\sigma)^2(2\pi)^1$. In the bent HCO molecule the π orbitals split into one a' and one a'' orbital. The possible combinations are compiled in Table I together with the correlating CO states. Table II compiles the computed data for the valence and Rydberg doublet and quartet states of the formyl radical at the ground state equilibrium geometry. More extensive theoretical studies of diabatic surfaces and conical intersections are available.^{27–31} The present calculations only aim at giving an accurate picture of the vertical absorption spectrum of the molecule.

The obtained CASPT2 results for the vertical excitation energies do not strongly differ from those reported previously^{26,32} for the low-lying states. The lowest excited state is computed to be the $\tilde{A}\ ^2A''$ state at 2.07 eV with an oscillator strength 0.002. The $\tilde{A}\ ^2A'' \leftarrow \tilde{X}\ ^2A'$ transition is known as the red absorption system⁵ and has been extensively studied. The $\tilde{A}\ ^2A''$ state has a linear equilibrium ge-

TABLE II. Calculated and experimental excitation energies (ΔE , eV), oscillator strengths (f), transition moment directions (TM_{dir} , °), dipole moments μ (D), and dipole moment directions (μ_{dir} , °), for the excited doublet and quartet states in HCO at the ground state equilibrium geometry.

State	Excitation energies			f	$\text{TM}_{\text{dir}}^{\text{a}}$	μ	$\mu_{\text{dir}}^{\text{a}}$	Other calculations		
	CAS	PT2	Expt					ΔE^{b}	ΔE^{c}	f^{c}
$1^2A'(\text{G.S.})^{\text{d}}$	1.62	+36
$1^2A''(7a' \rightarrow 2a'')^{\text{d}}$	3.39	2.07	2.0–2.2 ^e	0.002	...	1.33	+29	2.33	1.90	0.003
$2^2A'(7a' \rightarrow 3s)$	6.33	5.45	...	0.028	–11	3.10	+75	5.68	5.43	0.020
$1^4A''(6a' \rightarrow 2a'')$	6.68	6.19	0.54	+29	...	5.73	...
$3^2A'(6a' \rightarrow 7a')^{\text{d}}$	7.66	6.25	4.8–5.9 ^f	0.021	–37	1.29	–53	6.55	6.49	0.029
$4^2A'(7a' \rightarrow 3p_y)$	7.08	6.33	...	0.007	–39	1.41	+83	...	6.37	0.003
$5^2A'(7a' \rightarrow 3p_z)$	7.27	6.34	5.4–6.7 ^g	0.039	–56	4.62	+76	...	6.48	0.013
$2^2A''(7a' \rightarrow 3p_x)$	7.08	6.60	5.4–6.7 ^g	0.002	...	0.60	+87	7.00
$1^4A'(1a'' \rightarrow 2a'')$	8.24	6.70	0.72	–62	...	6.00	...
$3^2A''(1a'' \rightarrow 7a')^{\text{d}}$	7.62	7.06	...	0.003	...	1.88	–63	8.04	8.18	0.012
$4^2A''(6a' \rightarrow 2a'')$	9.07	7.56	...	0.016	...	0.52	–78	...	7.70	0.006
$6^2A'(1a'' \rightarrow 2a'')$	10.00	8.11	...	0.003	–66	1.00	–59	...	8.41	0.041
$2^4A''(5a' \rightarrow 2a'')$	9.64	8.88	1.18	–82

^aFor the relative definition of the angle see θ in Fig. 1.^bSelected CI calculations (Ref. 32).^cCI calculations (Ref. 26).^d $1^2A'$: \tilde{X}^2A' , $1^2A''$: \tilde{A}^2A'' , $3^2A'$: \tilde{B}^2A' , $3^2A''$: \tilde{C}^2A'' . See text.^eRed band system. It involves the weak \tilde{A}^2A'' state (Refs. 7, 8, 17).^fHydrocarbon flame bands. It mainly involves progressions of the \tilde{B}^2A' state (Ref. 21).^gAssigned to the transition to $3p^2\Pi$ in the linear molecule (Ref. 57).

ometry and strong vibronic coupling through a Renner–Teller interaction with the ground state and has been shown to have a rapid predissociation.¹⁰ The calculated vertical excitation energy of the second excited state, the $2^2A'$ $3s$ Rydberg state, is 5.45 eV and it has an oscillator strength of 0.028. This is in agreement with previous calculations. The $3s$ state has its global minimum at a linear geometry²⁹ and crosses with the \tilde{B}^2A' state along different paths. The role of the $3s$ state in the predissociation observed in the hydrocarbon flame bands of HCO was suggested by the early study of Bruna *et al.*²⁶ Recently calculations show the complex structure of the potential energy surfaces in this region.²⁹

The next doublet excited state in the vertical spectrum is the \tilde{B}^2A' valence state. The computed energy is 6.25 eV and the oscillator strength 0.021, close to that of the $3s$ state. It has been reported that, except for its lower vibrational states, the \tilde{B}^2A' state presents an important predissociative behavior for higher vibrational states.^{19–21} A recent laser induced fluorescence study by Lee and Chen²⁰ observed a decrease in the lifetimes of the \tilde{B}^2A' state with the increase in the rotation on the a axis, implying a Coriolis interaction leading to the continuum of another state, most likely the \tilde{A}^2A'' state, which is also strongly predissociating. An additional mechanism for predissociation was also suggested at even higher energy, maybe involving another state.²⁰ Dixon¹⁵ identified the transition observed in matrix at $41\,270\text{ cm}^{-1}$ as the origin of the \tilde{C}^2A'' state and Jacox¹⁸ assigned the observed progressions to vibrational levels of this state, which would have the fundamental frequencies 1200 cm^{-1} and 960 cm^{-1} for its second and third vibrational modes, respectively. More recent investigations^{21,22} show that these bands belong to the \tilde{B}^2A' state and can be as-

signed to progressions in one quanta of the first oscillator of the \tilde{B}^2A' state. The existence of the \tilde{C}^2A'' state below $42\,300\text{ cm}^{-1}$ has been questioned.²² Our vertical computed energy for the \tilde{C}^2A'' is 7.06 eV and the oscillator strength is 0.003. This excitation energy is lower than those previously computed, 8.18 eV (Ref. 26) and 8.04 eV (Ref. 32).

We have optimized the \tilde{C}^2A'' state by the fitting procedure. The resulting equilibrium geometry is CH bond length 1.114 Å , CO bond length 1.464 Å , and bond angle 101.6° . The computed harmonic frequencies are 2854 cm^{-1} , 1374 cm^{-1} , and 883 cm^{-1} , and correspond to the CH and CO stretchings and the HCO bending, respectively, changing the character of the second and third mode with respect to the \tilde{B}^2A' state. These results compare well to the UMP2 and CASSCF values reported by Francisco *et al.*⁴⁰ In all cases the CH bond and HCO angle values remain close to those of the \tilde{B}^2A' state and only the CO bond length increases (0.08 Å at the CASPT2 level). The most intense progression should be expected to involve the second mode in the absorption process. The computed energies are vertical 7.19 eV , T_e 5.17 eV , and T_0 5.13 eV . These results place the band origin for the \tilde{C}^2A'' state 0.5 eV (more than 4000 cm^{-1}) above the \tilde{B}^2A' origin. This result is in agreement with the experimental data, which suggest the \tilde{C}^2A'' origin should be at least $3\,650\text{ cm}^{-1}$ above the $38\,695\text{ cm}^{-1}$ transition (\tilde{B}^2A' origin), that is, higher than $42\,345\text{ cm}^{-1}$, discarding Dixon¹⁵ and Jacox's¹⁸ assignment. These energy differences do not rule out the possible role of the \tilde{C}^2A'' state on the predissociation mechanism of the \tilde{B}^2A' state.

We have computed other excited states which are believed not to have an important interaction with the \tilde{B}^2A'

TABLE III. Experimental and theoretical structural (\AA and deg) and spectroscopic constants (cm^{-1}) for the ground (\tilde{X}^2A') state of the HCO molecule.^a

	Experimental							Theoretical					
	M69 ^b	D69 ^c	A74 ^d	H86 ^e	M86 ^f	S90 ^g	T95 ^h	B86 ⁱ	C88 ^j	F92 ^k	M94 ^l	W95 ^m	Pres ⁿ
ω_1		2768			2790			2815	2825	3130	2660		2713
ω_2		1862			1920	1875		1903	1997	1989	1955		1877
ω_3		1093			1126	1101		1156	1159	1233	1182		1107
x_{11}		−140			−165				−86				−134
x_{22}					−17	−13	−12		−11				−13
x_{33}					−13	−14	−12		−11				−15
x_{12}					−22		1		1				3
x_{13}					−27		−49		−21				−7
x_{23}					−10	−4	−4		−2				−5
ν_1	2483				2440	2435	2435	2448	2642			2446	2443
ν_2	1863				1868	1868	1881	1885	1975			1844	1851
ν_3	1087				1081	1087	1093	1104	1126			1081	1072
r_{CH}			1.110	1.119				1.120	1.114	1.094	1.111	1.118	1.112
r_{CO}			1.171	1.175				1.195	1.175	1.178	1.188	1.182	1.183
$\text{H}\hat{\text{C}}\text{O}$			127.4	124.4				124.5	125.6	124.9	124.0	124.5	124.9

^aOrder of the oscillators: ν_1 CH stretching, ν_2 CO stretching, and ν_3 HCO bending.^bIR and UV spectra in CO and argon matrices (Refs. 4, 17).^cFit of matrix data including anharmonicities for the CH stretching (Ref. 16).^dMicrowave spectroscopy (Ref. 2).^e R_e parameters (Ref. 58). R_0 values measured 1.125 \AA , 1.175 \AA , and 125.0 deg, respectively (Ref. 8).^fPhotoelectron spectroscopy in gas phase (Ref. 64).^gLaser induced fluorescence in gas phase (Ref. 19).^hDispersed fluorescence in jet-cooled HCO (Ref. 24).ⁱSDCI+Q/DZP calculations. The ν 's were computed using an empirically corrected surface (Ref. 34).^jSDCI/TZP calculations. Anharmonicities SCF/TZP (Ref. 65).^kCASSCF/6-31+G* calculations (Ref. 40).^lCASSCF/SOCI/TZP calculations (Ref. 41).^mICII+Q/VQZ3P+2f calculations (Ref. 38).ⁿPresent CASPT2/VTZ2P+f calculations.

state. The Rydberg states to $3p$ -type orbitals are computed from 6.33 to 6.60 eV. The $^2A'$ ($3p_z$) state at 6.34 eV has the largest oscillator strength of the computed vertical spectrum, 0.039. This state forms a Renner–Teller pair together with the $3p_x$ state. It has been suggested that diffuse features observed more than 6000 cm^{-1} above the \tilde{B}^2A' origin correspond to a weak continuum underlying transition to the $3p^2\Pi$ linear state.⁵⁷

The mixing of the \tilde{X}^2A' state with the low-lying quartet state has also been considered as a possible explanation for the observed predissociation.¹⁹ A recent theoretical study by Manaa and Yarkony⁴¹ addressed the possibility of a spin–orbit induced perturbation of the low-lying vibrational levels of the \tilde{B}^2A' state due to the close presence of the $1^4A''$ state minimum only 1500 cm^{-1} above the \tilde{X}^2A' minimum. A weak spin–orbit interaction was found with the $1^4A'$ state, formally a double excitation from the \tilde{B}^2A' state. We have computed the vertical excitation to the $1^4A''$ state to be 6.19 eV. This is a valence state mainly described by the excitation $6a' \rightarrow 2a'$. The next quartet of the same symmetry is also a valence state computed at 8.88 eV (cf. Table II). The $1^4A'$ state, on the other hand, has been computed at 6.70 eV, somewhat higher than the previous CI calculation at 6.00 eV.²⁶ This state is not expected to play an important role in the \tilde{B}^2A' state photophysics.

Several experimental observations at low energy have been related to the states of the linear HCO (Ref. 29) and they will not be discussed here.

B. The ground \tilde{X}^2A' in HCO and its isotopomers

The lowest energy potential surface of the formyl radical has been the subject of several experimental and theoretical studies. Table III summarizes the most important experimental and theoretical structural and vibrational parameters for the ground (\tilde{X}^2A') state of the formyl radical molecule, together with the present CASPT2 values.

The ground state equilibrium geometry of HCO has an unusually long CH bond length. The value obtained by microwave spectroscopy is 1.110 \AA .² More recent investigations report a value for r_e of 1.119 \AA .⁵⁸ The dissociation energy along the CH stretching coordinate is consequently small, 18 kcal/mol.^{59,60} The bond length can be compared to the CH bond in H_2CO , 1.102 \AA .⁶ This is somewhat shorter since the new electron in formaldehyde is placed in the $7a'$ HCO orbital, which changes from C_{2p} to CH bond character in H_2CO . The measured values of the CO bond length and the HCO angle are 1.175 \AA (Ref. 8, 58) 125.0° (Ref. 8) and 124.4°,⁵⁸ respectively. All the theoretical studies on the formyl radical (cf. Table III) basically agree with the reported experimental data. The best agreement is obtained for the most recent calculations by Werner *et al.*³⁸ and the present CASPT2 results. Both are performed with high quality methods such as ICCI+Q and CASPT2. In both cases the CO length, 1.182 \AA and 1.183 \AA , respectively, is predicted to be almost 0.01 \AA larger than the available experimental value, 1.175 \AA . The results can be compared to the CO bond

TABLE IV. Experimental and theoretical spectroscopic constants (cm^{-1}) for the ground (\tilde{X}^2A') state of isotopically substituted HCO molecules.^a

	Experimental						Theoretical					
	M69 ^b	D69 ^c DCO	L81 ^d	D69 ^c C ¹³ CO	H86 ^e H ¹³ CO	D69 ^c HC ¹⁸ O	B86 ^f DCO	C88 ^g DCO	Present ^h			
									DCO	D ¹³ CO	H ¹³ CO	HC ¹⁸ O
ω_1		2068		2047			2054	2129	2025	2002	2705	2713
ω_2		1820		1789			1861	1929	1831	1803	1836	1831
ω_3		849		842			897	901	859	851	1100	1103
x_{11}		-58		-63		-139		-26	-51	-58	-133	-134
x_{22}								-8	-9	-9	-12	-12
x_{33}								-3	-10	-10	-15	-15
x_{12}								-44	-46	-30	3	3
x_{13}								-11	-9	-8	-7	-7
x_{23}								-14	0	1	-4	-4
ν_1	1926	1937	1910	1910	2437		2441	1930	2049	1894	1867	2437
ν_2	1803	1800	1795	1780	1829	1821	1824	1809	1883	1789	1770	1811
ν_3	850	852	847	845	1074	1084	1076	865	882	835	828	1065

^aOrder of the oscillators: ν_1 CH stretching, ν_2 CO stretching, and ν_3 HCO bending.^bIR and UV spectra in CO and argon matrices (Refs. 4, 17).^cFit of matrix data (Ref. 3) including anharmonicities for the CH stretching (Ref. 16).^dLaser magnetic resonance data (Ref. 69). Absorption spectroscopy for ν_3 (Ref. 8).^eFit of matrix data (Ref. 17) corrected for matrix shifts (Ref. 58).^fSDCI+Q/DZP calculations (Ref. 34).^gSDCI/TZP calculations. Anharmonicities SCF/TZP (Ref. 65).^hPresent CASPT2/VTZ2P+f calculations.

length in the CO molecule, 1.128 Å in the $X^1\Sigma^+$ ground state and 1.209 Å in the $a^3\Pi$ first excited state.⁶² The decrease in the bond length from 1.209 Å in the original $a^3\Pi$ state of CO to the \tilde{X}^2A' state of HCO can be understood as an electron leaving a CO antibonding orbital (cf. Table I). At the ground state CASPT2 optimized geometry the computed rotational constants are A_e 24.75 cm^{-1} , B_e 1.48 cm^{-1} , and C_e 1.40 cm^{-1} . These results are in good accord with recent experimental values,⁶³ A_0 24.33 cm^{-1} , B_0 1.49 cm^{-1} , and C_0 1.40 cm^{-1} .

The most recent experimental measurements of the HCO ground state vibrational fundamentals confirm the well-known character of each normal mode. The CH stretching fundamental has been measured to be ν_1 2440 cm^{-1} (Ref. 64) and 2435 cm^{-1} .^{10,19,24} The error interval is larger for the measured frequency of the CO stretching, ν_2 1868 cm^{-1} (Refs. 19, 64) and 1881 cm^{-1} .²⁴ Finally, the measured values for the fundamental frequency corresponding to the HCO bending mode ν_3 are 1081 cm^{-1} ,⁶⁴ 1087 cm^{-1} ,¹⁹ and 1093 cm^{-1} .²⁴ Comparing the experimental to the theoretical results, again the ICCI+Q (Ref. 38) and the CASPT2 values have the best overall agreement. The results of Werner *et al.*³⁸ are expected to be the most accurate, due to the number of geometries considered and the quality of the method. The theoretical results tend to support the 1868 cm^{-1} value for the CO stretching bond. In our calculation of the HCO ground state modes we observe that ν_1 and ν_3 can clearly be characterized as the CH stretching and HCO bending modes (95% and 97% in the composition of the eigenvectors, respectively), while ν_2 has 80% of contribution of the CO stretching and 19% of the HCO bending. The comparison to the harmonic frequencies is not so favorable. The error bars in this case are very large. The harmonic frequency for the bending mode, ω_3 has been reported by experiment at

1093 cm^{-1} (matrix),¹⁶ 1126 cm^{-1} ,⁶⁴ and 1101 cm^{-1} .¹⁹ On the other hand, the reported values for the CO mode are 1862 cm^{-1} (matrix),¹⁶ 1920 cm^{-1} ,⁶⁴ and 1875 cm^{-1} .¹⁹ All the previous theoretical studies obtain values for these parameters even larger than the largest experimental value (except Bowman *et al.*³⁴ for ω_2). The CASPT2 results agree well with the most recent laser induced fluorescence study of Sappey and Crosley.¹⁹ The overall disagreement is larger for the CH stretching harmonic frequency. The previous theoretical values, except for the CASSCF/SOCI calculations by Manaa and Yarkony,⁴¹ are too high while CASPT2 computes a low value of 2713 cm^{-1} . It is not surprising that the anharmonicity term is most important for the CH stretching mode. Dixon¹⁶ estimated x_{11} to be -140 cm^{-1} and Murray *et al.*⁶⁴ -165 cm^{-1} . These values can be compared to -86 cm^{-1} computed by Clabo *et al.*⁶⁵ and -134 cm^{-1} computed for the CASPT2 surface. The large anharmonic correction in the CH stretching frequencies (between 200 cm^{-1} and 350 cm^{-1}) is a consequence of the weakness of the CH bond and the low energy dissociation channel.

Table IV compiles the experimental and theoretical data for several isotopically substituted HCO molecules. To compute our values we have made the assumption that the equilibrium geometry does not change upon isotopic substitutions. As expected, the largest observed and computed isotope shifts are for ν_1 , CH (CD) stretching, on deuteration. The agreement between theoretical and experimental values is good once matrix effects have been considered. On deuteration, the value of x_{11} decreases dramatically, as well as the whole role of the CH (CD) anharmonicity in the vibrational spectrum. Regarding the other anharmonic constants, due to spectral congestion⁶⁴ no experimental values have been reported for the ground state of DCO except the data

TABLE V. Experimental and theoretical structural (Å and deg) and spectroscopic constants (cm⁻¹) for the excited \tilde{B}^2A' state of the HCO and DCO molecules.^a

	HCO								DCO	
	Experimental					Theoretical			Expt Theo	
	D69 ^b	M69 ^c	C92 ^d	A93 ^e	S94 ^e	T79 ^f	F92 ^g	M94 ^h	Pres ⁱ	C92 ^d Pres ⁱ
ω_1			2798				3125	2933	2825	2069 2072
ω_2			1412				1209	1448	1400	1240 1210
ω_3			1107				1510	1127	1081	944 945
x_{11}			-76						-96	-48 -52
x_{22}			5						-9	-7 -4
x_{33}			-9						-12	-4 -8
x_{12}			-64						-3	-26 -9
x_{13}			-33						31	-30 4
x_{23}			-16						-13	1 -8
ν_1			2597		2596				2646	1944 1965
ν_2		1375	1382		1381				1386	1213 1193
ν_3		1035	1066		1066				1056	922 924
T_0	38691		38695	38695	38696	31858		37511	37325	38628 37503
r_{CH}	1.16					1.154	1.097	1.110	1.110	
r_{CO}	1.36					1.460	1.371	1.384	1.382	
\hat{HCO}	111					103.0	106.1	105.1	104.6	

^aOrder of the oscillators: ν_1 CH stretching, ν_2 HCO bending and ν_3 CO stretching. The same assignment for DCO.

^bValues in argon matrix. The CH distance is an assumed value (Ref. 15).

^cMatrix-isolation values (Ref. 17).

^dResonance ionization spectroscopy in jet-cooled HCO (Ref. 21).

^eFluorescence excitation spectrum in gas phase (A93) (Ref. 22) and in supersonic jet (S94) (Ref. 23).

^fSelected SDCl calculations. T_0 is here T_e (Ref. 32).

^gCASSCF/6-31+G* calculations (Ref. 40).

^hCASSCF/SOCI/TZP calculations. T_0 is here T_e (Ref. 41).

ⁱPresent CASPT2/VTZ2P+f calculations.

from Dixon,¹⁶ which only include CH stretching anharmonicities. A large value for x_{12} is observed even using such an approach (-32 cm⁻¹). The same conclusion is obtained by Clabo *et al.*⁶⁵ who compute a value of -44 cm⁻¹. The CASPT2 values for x_{12} in DCO is -46 cm⁻¹ and -30 cm⁻¹ for D¹³CO. This is a consequence of the enhanced mixing of the CO and CD stretches in DCO due to the proximity of ν_1 and ν_2 . The vibrational constants for other isotopomers such as H¹³CO or HC¹⁸O do not strongly vary from the HCO ground state values.

C. The excited \tilde{B}^2A' state in HCO and DCO

Table V lists the available experimental and theoretical structural and spectroscopical parameters for the excited \tilde{B}^2A' state of the HCO and DCO molecules, including the present CASPT2 computed values. The only experimental value of the equilibrium geometry of the valence \tilde{B}^2A' excited state is the old estimate of Dixon,¹⁵ obtained by fitting of the rotational parameters. The CO bond length was determined to be 1.36 Å and the HCO angle 111°. Noting that there was no evidence for excitation of the CH stretching fundamental in the analyzed bands, Dixon assumed that the CH bond had the same length in both the ground and the excited state. He used a value of 1.16 Å, which has been proved to be too long. The assumption that the CH length does not basically change from the ground to the excited state seems to be confirmed by the CASPT2 calculations, which compute values of 1.112 and 1.110 Å, respectively.

As seen in Table I the CH bond is not involved in the excitation $\tilde{B}^2A' \leftarrow \tilde{X}^2A'$. Dixon's estimate¹⁵ of the CO bond length is in good agreement with the CASPT2 computed value of 1.382 Å. This is considerably longer than in the ground state, a fact also reflected in the orbital composition. The excited electron goes from a CO bonding orbital in the ground state to a CO antibonding orbital in the excited state. The HCO radical is also more bent than in the ground state. The CASPT2 computed value of 104.6° is even smaller than the estimated value of 111°. Previous theoretical calculations on the \tilde{B}^2A' state geometry were performed with poorer methods or basis sets^{32,40} and some discrepancies with the CASPT2 results are appreciable (cf. Table V). The agreement is better with the CASSCF/SOCI results of Manaa and Yarkony.⁴¹ At the \tilde{B}^2A' CASPT2 optimized excited state geometry the computed rotational constants are $A_e 16.38$ cm⁻¹, $B_e 1.18$ cm⁻¹, and $C_e 1.10$ cm⁻¹. These results are in good accord with the most recent experimental values,²⁰ $A_0 16.00$ cm⁻¹, $B_0 1.16$ cm⁻¹, and $C_0 1.07$ cm⁻¹.

Milligan and Jacox¹⁷ assigned the ν_2 vibrational levels of the \tilde{B}^2A' excited state obtained at 1375 cm⁻¹ for HCO and 1150 cm⁻¹ for DCO to the bending mode, and the ν_3 vibrational levels at 1035 cm⁻¹ in HCO and 925 cm⁻¹ in DCO to the CO stretching mode. Their assignment was based on the strong argument that substitution of hydrogen by deuterium could hardly decrease the CO stretching frequency by 225 cm⁻¹ if ν_2 was the CO stretching mode. In addition, they observed how deuterium substitution enhanced

the development of progressions in ν_2 , supposedly involving appreciable hydrogen or deuterium atom motion. Cool and Song²¹ agree with this assignment and reinforce it by arguing that for a bent triatomic molecule excitation of the bending vibration always causes a much larger increase in the A rotational constant than excitation on any stretching vibration, which is known to be a safe criterion.²² Sappey and Crosley¹⁹ favor, however, the opposite assignment without clear arguments. The only, to our knowledge, theoretical study of the vibrational frequencies for the \tilde{B}^2A' state of HCO was reported by Francisco *et al.*⁴⁰ at a CASSCF/6-31+G* level of calculation. They assigned their computed 1510 cm^{-1} frequency to the CO stretching mode and the 1209 cm^{-1} frequency to the HCO bending mode, in agreement therefore with Sappey and Crosley. Considering that both Francisco's and our own CASPT2 theoretical calculations lead to similar geometries for the \tilde{B}^2A' state, their result is somewhat surprising. We have obtained the opposite assignment. The CASPT2 fundamental frequencies for the \tilde{B}^2A' state of the HCO molecule are ν_1 , 2646 cm^{-1} , ν_2 1386 cm^{-1} , and ν_3 1056 cm^{-1} . The corresponding assignments are CH stretching, HCO bending, and CO stretching, respectively, in agreement with Milligan and Jacox¹⁷ and with Cool and Song.²¹

Adamson *et al.*²² also agree with this latter assignment, although they leave some open questions waiting for a proper normal mode analysis. For instance, similar HCO/DCO isotope shifts have been observed in both modes; 14% for ν_2 and 12% for ν_3 (cf. Table V). In addition, a large change in the CO stretching frequency is observed from the ground state fundamental frequency, 1851 cm^{-1} , to the excited state value, 1056 cm^{-1} (CASPT2 values). These frequencies would correspond to bond orders of 2.5 and 1, respectively. This is an unexpectedly large decrease upon nominal promotion of a single electron. This can be partially explained by the double occupation of the $7a'$ orbital, which has a clear CO antibonding character, in the \tilde{X}^2A' state. The increase of the HCO bending frequency can also be considered to be an effect of the increased in-plane repulsion on the occupation of $7a'$. In our harmonic normal mode analysis we have found the suggested²² mixed character of the second and third modes in the \tilde{B}^2A' state, especially in the DCO system, which might account for the remaining isotope and state shifts in the vibrational frequencies. For the \tilde{B}^2A' state of the HCO molecule the ν_2 mode has 25% and 74% of contribution of CO stretching and HCO bending, respectively, in the composition of the eigenvector. The percents change to 66% and 28% for the ν_3 mode. The mixing is more severe in DCO, where the modes have almost equal contribution from both CO stretching and HCO bending coordinates. Cool and Song²¹ were unable to find the clear behavior of the rotational parameters in DCO as they did in HCO.

The CASPT2 values for the vibrational frequencies and anharmonicity constants in the \tilde{B}^2A' state of HCO agree with the values reported by the resonance two-photon ionization study of Cool and Song.²¹ The overall agreement is even better for the DCO system. The fundamental frequencies

suggest strong Fermi resonances between ν_1 and $2\nu_2$, in HCO and between ν_1 and $2\nu_3$ in DCO. The anharmonicity constant x_{11} for HCO strongly decreases from the ground state value both in experiment and in the CASPT2 theoretical study. The coupling between the first and the other modes is, however, expected to remain. Cool and Song²¹ reported large values for the x_{12} and x_{13} anharmonicity constants both in the ground (-22 cm^{-1} and -27 cm^{-1} , respectively) and excited (-64 cm^{-1} and -33 cm^{-1}) state. Our CASPT2 values are smaller in all the cases. The same effect is not observed for DCO. The reported x_1 value of -58 cm^{-1} (Ref. 16) in the ground state (-51 cm^{-1} from CASPT2) does not change much in the excited \tilde{B}^2A' state; -48 cm^{-1} (Ref. 21) (-52 cm^{-1} by CASPT2). The anharmonicity constants x_{22} and x_{33} remain smaller in all the cases. In general, the effects of the anharmonicity are smaller in the excited state than in the ground state and they are also smaller in DCO than in HCO.

D. The $\tilde{B}^2A' \leftarrow \tilde{X}^2A'$ absorption in HCO and DCO

The matrix isolation absorption spectra of Milligan and Jacox in 1969 (Ref. 17) is one of the most complete sources of vibrational data for the HCO \tilde{B}^2A' excited state. This spectrum is not affected by the severe predissociation effects that those obtained through laser techniques in gas phase or jet-cooled HCO are. They observed 38 absorption bands in the 210–260 nm region. The upper levels for 26 of these bands could be assigned to the HCO \tilde{B}^2A' state CO stretching and HCO bending overtones and combinations. The spectrum exhibited the expected strong progressions in the ν_2 and ν_3 vibrations caused by the large decreases in the CO bond length and HCO angle (0.2 Å and 20.3°, respectively, at the CASPT2 level) on excitation from the ground state. The upper states of most of the remaining 12 bands that Milligan and Jacox did not assign, could be understood as bending and CO stretch progressions built on an origin approximately 2500 cm^{-1} above the \tilde{B}^2A' state origin. They speculated that these bands might correspond to progressions built on one quantum of the \tilde{B}^2A' state CH stretch. Only recently Cool and Song²¹ observed and assigned the DCO counterparts of such bands confirming the early suggestion and ruling out Dixon's¹⁵ proposal that these bands were progressions in the \tilde{C}^2A'' state. Adamson *et al.*²² recently reported that the rotational contours of the bands at 41 278 cm^{-1} and 42 305 cm^{-1} were indistinguishable from the rotational contour of the band of the origin, i.e., a hybrid a , b -type band belonging to a state of A' symmetry. Our calculations place the \tilde{C}^2A'' state origin more than 4000 cm^{-1} above the \tilde{B}^2A' state origin, confirming the most recent findings.

Table VI compiles the experimentally observed vibrational levels for the excited \tilde{B}^2A' state of the HCO molecule together with our computed values. We have chosen our (000) transition to be the experimental gas-phase value 38 695 cm^{-1} .²¹ No scaling or any other changes has been applied to the computed values shown in Table VI. The obtained *ab initio* values, together with our computed vibra-

TABLE VI. Experimental and theoretical vibrational levels (cm^{-1}) for the excited \tilde{B}^2A' state of the HCO molecule.

Level	MJ69 ^a	SC90 ^b	CS92 ^c	SC94 ^d	Calc ^e	Level	MJ69 ^a	Calc ^e
000	38 567		38 695	38 696	38 695	023	44 510	44 481
001	39 623		39 760	39 761	39 751	006	44 829	44 771
010	39 956		40 075	40 076	40 081	032	44 829	44 797
002	40 655	40 807	40 809	40 809	40 789	112		44 820
011	41 005	41 122	41 125	41 125	41 124	201		44 844
100		41 290	41 292	41 292	41 342	041	45 153	45 099
020	41 344	41 470	41 468	41 468	41 443	015		45 123
003	41 689	41 845	41 841	41 841	41 811	121		45 178
012	42 022	42 155	42 158		42 159	210		45 242
101		42 325	42 324		42 394	050		45 385
021	42 342		42 501		42 472	104		45 448
110	42 468 ^f	42 600	42 609		42 758	024	45 502 ^f	45 459
030	42 722 ^f		42 854 ^f		42 781 ^f	130		45 520
004			42 984 ^f		42 815 ^f	007		45 724
013	43 053		43 175		43 157	033	45 815	45 780
102					43 429	113		45 825
022	43 352				43 485	202		45 876
200			43 736		43 795	300		46 055
111	43 503 ^f		43 626		43 798	016		46 079
031	43 808				43 798	042	46 175	46 086
005					43 801	051	46 519	46 376
040	44 039 ^f				44 095 ^f	025		46 420
014					44 149	034	46 780 ^f	46 269
120			43 935		44 151	043	47 133	47 055
103					44 447	052	47 468	47 350

^aAbsorption data on CO matrix (Ref. 17).^bLaser induced fluorescence data on gas phase (Ref. 19).^cResonance two-photon ionization in jet-cooled HCO (Ref. 21).^dLaser induced fluorescence data on supersonic molecular jet (Ref. 23).^ePresent CASPT2/VTZ2P+f calculations. The (000) transition is taken from experiment. The *ab initio* value is $37\,325\text{ cm}^{-1}$.^fNew or confirmed assignment. See text.

tional intensities, can be of some help in suggesting or confirming assignments in the bands.

Figure 1 shows our computed vibrational intensities for the low-energy part of the transition $\tilde{B}^2A' \leftarrow \tilde{X}^2A'$ (000) in the HCO molecule. The variational method explained in Sec. II B was used here. The figure includes transitions to vibrational states up to four quanta ($v_1 + v_2 + v_3 = 4$) in the normal modes. Figure 2 includes transitions to vibrational states up to seven quanta ($v_1 + v_2 + v_3 = 7$) in the normal modes, and has been computed using the harmonic approximation, in which the anharmonic corrections are considered in the position of the vibrational transitions via the usual perturbative expressions. The results obtained from the two methods are very similar, except that the transitions related to the first mode, CH stretching, (100), (101), and (110) have gained intensity when computed with the variational method (Fig. 1). The large effect of the anharmonicities related to the CH stretching might be considered to be the reason of such a discrepancy. If we compare the obtained transitions in Fig. 2 to the experimental spectra we find the best agreement with Milligan and Jacox's¹⁷ matrix data.

As displayed in Fig. 2 the most intense progressions of the HCO absorption spectrum to the \tilde{B}^2A' state are built on one, two, and three quanta in v_3 and on four and three quanta in v_2 . The transition to the level (042) is the most intense one in the computed spectrum. This description agrees well with the matrix spectrum reported by Milligan and Jacox,¹⁷

except for the (022) transition which was described by them as a weak shoulder. In Table VI we have assigned some of the bands Milligan and Jacox left unassigned. Transitions at $42\,468\text{ cm}^{-1}$ and $43\,503\text{ cm}^{-1}$ can be assigned to progressions in one quanta in v_1 which were not considered by Milligan and Jacox. Transitions reported at $45\,502\text{ cm}^{-1}$ and $46\,780\text{ cm}^{-1}$ are here assigned to the (024) and (034) levels, respectively, for the first time. We have reassigned two transitions. The band reported at $42\,722\text{ cm}^{-1}$ in the CO matrix¹⁷ and at $42\,854\text{ cm}^{-1}$ in the jet-cooled spectrum²¹ is assigned to the (030) level instead of the (004) level based on the larger intensity of the transition to the (030) level. As discussed by Cool and Song²¹ both assignments were consistent with the obtained data. The assignment was already suggested by Jacox.¹⁸ In this context we assign the band reported at $42\,984\text{ cm}^{-1}$ by Cool and Song to the transition to the (004) level. Another new assignment based on the computed intensity is performed for the transition to the (040) level reported at $44\,039\text{ cm}^{-1}$, which was previously assigned to the (014) level.

Figure 3 shows the computed vibrational intensities for the transition $\tilde{B}^2A' \leftarrow \tilde{X}^2A'$ (000) of the DCO molecule. The harmonic approach has been used in this case, as the variational method to not give any significant improvements. Note that the spectrum is plotted twice; in the second plot, the intensities have been magnified 1000 times, to show the weaker bands. For DCO it is the progression $(0v_20)$ in v_2

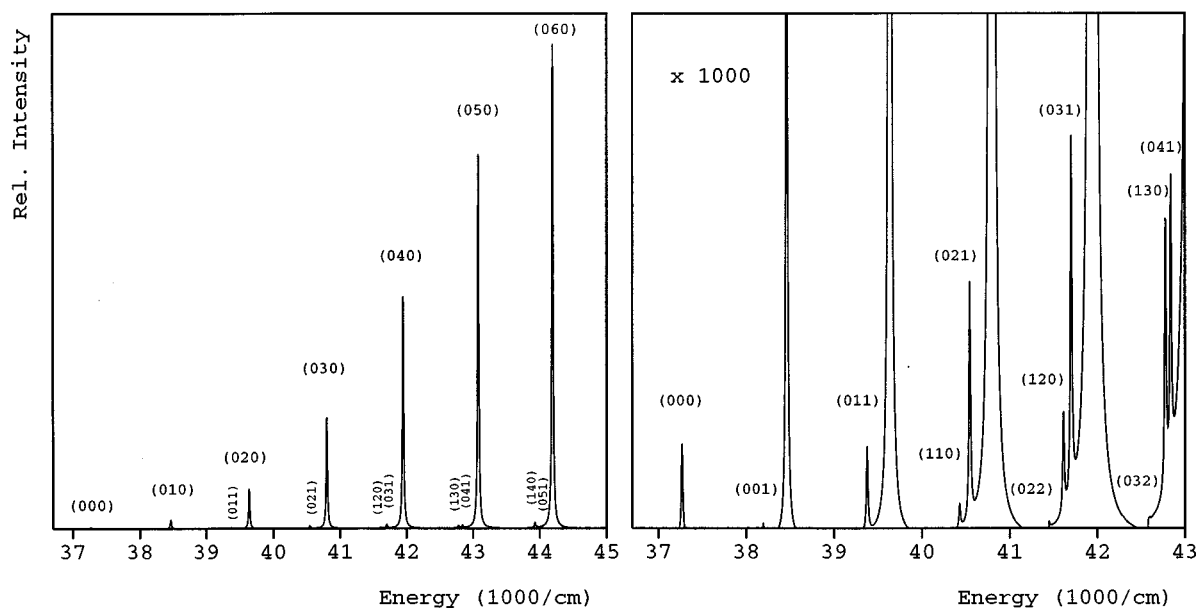


FIG. 3. Computed vibrational intensities for the absorption $\tilde{B}^2A' \leftarrow \tilde{X}^2A'$ (000) in DCO up to seven quanta ($v_1 + v_2 + v_3 = 7$). To the right, the intensities have been magnified 1000 times.

spectrum is severely affected by predissociation effects above this energy. Again, as in the HCO absorption spectrum, bands as (100), (101), and (110) are too weak in the computed spectrum.

E. The $\tilde{X}^2A' \leftarrow \tilde{B}^2A'$ emission in HCO

Figure 4 displays the computed vibrational transitions

for the emission process, $\tilde{X}^2A' \leftarrow \tilde{B}^2A'$ (000), in the HCO molecule with up to nine quanta ($v_1 + v_2 + v_3 = 9$). The harmonic approach was used. They can be compared to the 0_0^0 disperse fluorescence (DF) spectrum reported by Tobiason *et al.*²⁴ Upon excitation to the \tilde{B}^2A' state the large increase in the CO bond length and decrease in the HCO bond angle leads to a spectrum with long progressions in v_2 in combi-

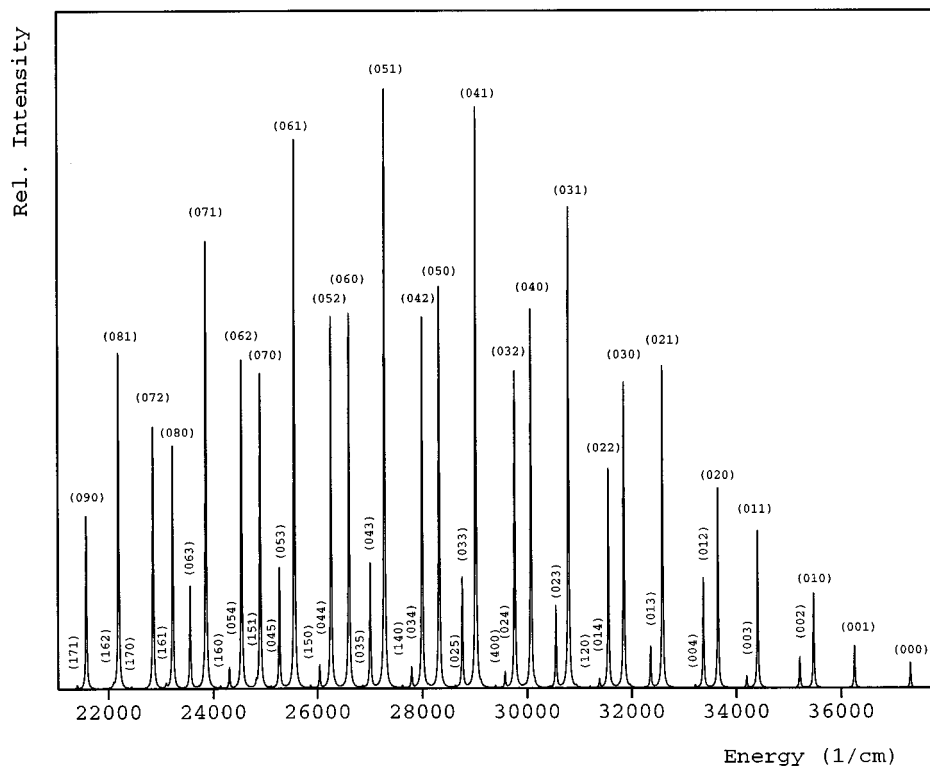


FIG. 4. Computed vibrational intensities for the emission $\tilde{X}^2A' \leftarrow \tilde{B}^2A'$ (000) in HCO up to nine quanta ($v_1 + v_2 + v_3 = 9$).

nation with the bend (note that the labels change from the \tilde{B}^2A' modes where ν_2 corresponded to the angle bending mode). No activity is expected in the CH stretch because of the small change in the CH bond length. These tendencies are observed both in the 0_0^0 DF (Ref. 24) and in our computed spectrum. Comparing the relative intensities Tobiasson *et al.*²⁴ found the most intense progressions for the $(0\nu_2\nu_3)$ series, decreasing in intensity as ν_3 goes from 0 to 3. We have found the most intense progression for $(0\nu_21)$, and the intensity then decreases as ν_3 goes from 1 to 3.

The previous experimental observations are in agreement with those reported by Dixon¹⁵ and Adamson *et al.*²² Dixon¹⁵ assigned four vibrational progressions in his hydrocarbon flame band emission spectrum. Vaidya's notation¹² was used and the progressions were called A_0 , A_1 , B , and short wavelength progressions, the two latter being related to higher vibrational levels of the initial state. The A_0 progression was assigned to the emission series $2_0^03_1^0$, i.e., (001), (011), (021),.... All these bands were found to be slightly diffuse. The A_1 progression was assigned to 2_0^0 ; (000), (010), (020),.... The bands belonging to this series were reported as sharp. Adamson *et al.*²² in their stimulated emission pumping (SEP) spectrum confirmed the assignments of Dixon.¹⁵ The diffuseness of the A_0 band was attributed to predissociation in the lower electronic state. In our theoretical spectrum the A_0 progression is the most intense one because the predissociation effects are not considered.

For the sake of brevity we will not present the computed vibrational levels for the ground \tilde{X}^2A' state of the HCO molecule. They can be obtained from the authors upon request. The more extensive calculations by Keller *et al.*⁶⁶ can be taken as reference for the assignments. In general the agreement between both calculations is good except for the states with higher quanta on ν_1 .

The direction of the transition dipole moment, $\mu_{\tilde{B}\tilde{X}}$, in the transition $\tilde{B}^2A' \leftrightarrow \tilde{X}^2A'$ of the HCO molecule has been reported from experiment to form an angle of ± 31 – 34° ,²² ± 41 – 44° ,²⁰ and $+39 \pm 2^\circ$ (Ref. 67) with respect to the inertial a axis of the system. The determination of the relative direction of $\mu_{\tilde{B}\tilde{X}}$ with respect to the CH or CO bonds is however uncertain.²² At the \tilde{B}^2A' state equilibrium geometry Manaa and Yarkony⁴¹ computed a transition dipole moment of 0.429 a.u. forming an angle of $+34.4^\circ$ with the inertial a axis. Our CASSCF results are 0.474 a.u. and $+30.3^\circ$, respectively. The inertial a axis for this geometry lies 4.8° away from the axis containing the CO bond towards the axis containing the CH bond (see Fig. 2 in Ref. 41 for the orientation of the axis). Therefore, $\mu_{\tilde{B}\tilde{X}}$ makes an angle of 79.2° from the CH bond, almost perpendicular to it. At the ground state equilibrium geometry we obtain similar results; a transition dipole moment of 0.433 a.u. and an angle of $+46.0^\circ$ with respect to the a axis, which lies in this case 6.3° away from the CO bond axis. We conclude then that the transition dipole moment for the $\tilde{B}^2A' \leftrightarrow \tilde{X}^2A'$ transition is almost perpendicular to the CH bond and the transition cannot be characterized exclusively as a or b -type (there is an angle of 25.4° with respect to the CO bond at the excited state equilibrium geometry). Both CO and CH bonds are

important contributors to the chromophore in the HCO molecule for the \tilde{B}^2A' state.

Lee and Chen²⁰ estimated the electronic transition dipole moment to be lower than 0.31 a.u. They measured a fluorescence lifetime of 89 ns for the $\tilde{X}^2A'(000) \leftarrow \tilde{B}^2A'(000)$ emission and applied the approximate relation $\tau^{-1}(\text{s}^{-1}) = 2.0261 \times 10^{-6} \nu_{\tilde{B}\tilde{X}}^3 \mu_{\tilde{B}\tilde{X}}^2$, where $\nu_{\tilde{B}\tilde{X}}$ is T_0 (in cm^{-1}) to obtain an upper bound for the transition dipole moment. Both Manaa and Yarkony⁴¹ and our own calculations obtain a larger value for $\mu_{\tilde{B}\tilde{X}}$. By using the previous expression, the pure radiative lifetime of the \tilde{B}^2A' state is computed to be 46.2 ns by Manaa and Yarkony, and 42.3 ns by us (we have used our own computed T_0). Meier *et al.*⁶⁸ measured 43 ns for the \tilde{B}^2A' collision free lifetime.

IV. SUMMARY AND CONCLUSIONS

The present paper reports CASSCF/CASPT2 ab initio calculations on different electronic states of the formyl radical, HCO, and several of its isotopomers. The CASPT2 method is here shown to be a robust correlation method comparable to extensive CI methods and it is the most accurate method applied to the excited states of the HCO system.

The absorption spectrum of HCO has three groups of bands from 2.0 to 6.7 eV. The red-bands system observed at 2.0–2.2 eV (Refs. 7, 8, 17) is related to the $1^2A''(\tilde{A}^2A'')$ valence state computed to be 2.07 eV at the CASPT2 level in the vertical spectrum as a weak transition. The second set of transitions is known as the hydrocarbon flame bands, detected at 4.8–5.9 eV.²¹ They mainly involve progressions of the $3^2A'(\tilde{B}^2A')$ state, computed at 6.25 eV in the vertical spectrum (6.10 eV if we used the fitted surface) with an oscillator strength of 0.021. A final group of transitions is observed at 5.4–6.7 eV.⁵⁷ They are assigned to the transition to the $3p^2\Pi$ state in the linear molecule. The present vertical results basically agree with the previously reported CI calculations for the available states,^{26,32} except for the highest states.

Through the calculation and fitting of both the ground \tilde{X}^2A' and \tilde{B}^2A' excited states surfaces for HCO and its isotopomers, we have obtained an accurate set of theoretical vibrational frequencies for these systems. The obtained CASPT2 optimized geometry for the HCO ground \tilde{X}^2A' state, 1.112 Å, C–H bond, 1.183 Å, C–O bond, and 124.9° , HCO angle, is consistent with the measured experimental and previously computed theoretical values. The normal mode analysis of the HCO ground state leads to the following set of fundamental frequencies and assignments: ν_1 2443 cm^{-1} , CH stretching; ν_2 1851 cm^{-1} , CO stretching, ν_3 1072 cm^{-1} , HCO bending. These values are in good agreement with the most recent gas-phase experimental data, 2435 cm^{-1} , 1868–1881 cm^{-1} , and 1087–1093 cm^{-1} ,^{19,24} respectively, and the agreement with the most accurate of the previous theoretical studies³⁸ is also good. This is also the case for the anharmonic analysis. The x_{11} anharmonic correction, related to the CH stretching mode, was estimated to have a large value between -140 cm^{-1} and -165 cm^{-1} ,^{15,64} which agrees with our computed value of -134 cm^{-1} . Upon deuteration the anharmonicity effects on the CH stretching

decreases. Consequently, the x_{11} value is computed to be -51 cm^{-1} in DCO, in agreement with the experimental estimate of -58 cm^{-1} . The agreement between our computed and the experimental fundamental, harmonic, and anharmonic frequencies is good for all the isotopomers of HCO.

The obtained geometry for the \tilde{B}^2A' excited state of HCO, 1.110 Å, C–H bond; 1.382 Å, C–O bond, and 104.6° , HCO angle, agrees with the most accurate of the previous theoretical calculations.⁴¹ There is no accurate experimental determination of the geometry of the state although it is known that the CO bond and the HCO angle should drastically increase and decrease, respectively, upon excitation. This is consistent with our computed results. Strong progressions on the modes related to the CO bond and the HCO angle should be expected in the absorption and emission spectra. This work contains the first theoretical calculations of the fundamental frequencies of the HCO \tilde{B}^2A' state. The computed frequencies and their assignments are ν_1 2646 cm^{-1} , CH stretching; ν_2 1386 cm^{-1} , HCO bending, and ν_3 1056 cm^{-1} , CO stretching. The agreement with the experimental values 2597 cm^{-1} , 1382 cm^{-1} , and 1066 cm^{-1} ,²¹ respectively, is good for the second and third fundamentals, but less so for ν_1 , probably due to the major role of the anharmonic effects, which are difficult to compute accurately for this system. Our normal mode analysis, however, led to the conclusion that the second mode should be assigned to the HCO bending and the third mode to the CO stretching. This assignment agrees with the analysis performed by Milligan and Jacox,¹⁷ Cool and Song,²¹ and Adamson *et al.*,²² but disagrees with the less clear results of Sappey and Crosley¹⁹ and the only previous theoretical results of Francisco *et al.*⁴⁰ For DCO the analysis is more complex. Although the agreement between our computed data and the only experimental available data²¹ are better than in HCO, the normal mode analysis is inconclusive due to mode mixing.

Finally, the vibrational intensities of the absorption (HCO and DCO) and emission process $\tilde{B}^2A' \leftrightarrow \tilde{X}^2A'$ have been computed and some of the observed bands have been assigned and compared with previous assignments. There is a general agreement in the obtained intensities of the bands, especially in the absorption spectrum in matrix by Milligan and Jacox¹⁷ which does not suffer so severely from predissociation effects as do the jet-cooled and the gas-phase laser studies. Our calculation of the \tilde{C}^2A'' state origin more than 4000 cm^{-1} above the \tilde{B}^2A' state origin confirms also the assignment²² of the transitions of the \tilde{B}^2A' spectrum related to one quantum of the first mode and rules out the participation of the \tilde{C}^2A'' state in the low-lying progressions of the hydrocarbon flame bands of HCO. The transition dipole moment direction has been also computed to be almost perpendicular to the CH bond.

ACKNOWLEDGMENTS

The research reported in this paper has been supported by a grant from the Swedish Natural Science Research Coun-

cil (NFR), by project PB94-0986 of the DGICYT of Spain, and by the European Commission through the TMR network FMRX-CT96-0079.

- ¹J. D. Tobiasson and E. A. Rohlfing, Chem. Phys. Lett. **333**, 342 (1996).
- ²J. A. Austin and D. H. Levy, J. Chem. Phys. **60**, 207 (1974).
- ³G. E. Ewing, W. Thompson, and G. C. Pimentel, J. Chem. Phys. **32**, 927 (1960).
- ⁴D. E. Milligan and M. E. Jacox, J. Chem. Phys. **41**, 3032 (1964).
- ⁵D. A. Ramsay, J. Chem. Phys. **21**, 960 (1953).
- ⁶G. Herzberg and D. A. Ramsay, Proc. R. Soc. London, Ser. A **233**, 34 (1955).
- ⁷J. W. C. Johns, S. H. Priddle, and D. A. Ramsay, Discuss. Faraday Soc. **35**, 90 (1963).
- ⁸J. M. Brown and D. A. Ramsay, Can. J. Phys. **53**, 2232 (1975).
- ⁹R. König and J. Lademann, Chem. Phys. Lett. **94**, 152 (1983).
- ¹⁰B. M. Stone, M. Noble, and E. K. C. Lee, Chem. Phys. Lett. **118**, 83 (1985).
- ¹¹G. Rumbles, J. J. Valentini, B. M. Stone, and E. K. C. Lee, J. Phys. Chem. **93**, 1303 (1989).
- ¹²W. M. Vaidya, Proc. R. Soc. London, Ser. A **147**, 513 (1934).
- ¹³W. M. Vaidya, Proc. Phys. Soc. **64**, 428 (1951).
- ¹⁴W. M. Vaidya, Proc. R. Soc. London, Ser. A **279**, 572 (1964).
- ¹⁵R. N. Dixon, Trans. Faraday Soc. **65**, 3141 (1969).
- ¹⁶R. N. Dixon, J. Mol. Spectrosc. **30**, 248 (1969).
- ¹⁷D. E. Milligan and M. E. Jacox, J. Chem. Phys. **51**, 277 (1969).
- ¹⁸M. E. Jacox, Chem. Phys. Lett. **56**, 43 (1978).
- ¹⁹A. D. Sappey and D. R. Crosley, J. Chem. Phys. **93**, 7601 (1990).
- ²⁰S. H. Lee and I. C. Chen, J. Chem. Phys. **103**, 104 (1995).
- ²¹T. A. Cool and X. M. Song, J. Chem. Phys. **96**, 8675 (1992).
- ²²G. W. Adamson, X. Zhao, and R. W. Field, J. Mol. Spectrosc. **160**, 11 (1993).
- ²³Y. J. Shiu and I. C. Chen, J. Mol. Spectrosc. **165**, 457 (1994).
- ²⁴J. D. Tobiasson, J. R. Dunlop, and E. A. Rohlfing, J. Chem. Phys. **103**, 1448 (1995).
- ²⁵A. D. Walsh, J. Chem. Soc. **1953**, 2288.
- ²⁶P. Bruna, R. J. Buenker, and S. D. Peyerimhoff, J. Mol. Struct. **32**, 217 (1976).
- ²⁷M. Perić and S. D. Peyerimhoff, J. Mol. Struct. **297**, 347 (1993).
- ²⁸M. Perić and S. D. Peyerimhoff, J. Chem. Phys. **98**, 3587 (1993).
- ²⁹H. Lorenzen-Schmidt, M. Perić, and S. D. Peyerimhoff, J. Chem. Phys. **98**, 525 (1993).
- ³⁰M. Staikova, M. Perić, B. Engels, and S. D. Peyerimhoff, J. Mol. Spectrosc. **166**, 423 (1994).
- ³¹M. Perić, C. M. Marian, and S. D. Peyerimhoff, J. Mol. Spectrosc. **166**, 406 (1994).
- ³²K. Tanaka and E. R. Davidson, J. Chem. Phys. **70**, 2904 (1979).
- ³³T. H. Dunning, J. Chem. Phys. **73**, 2304 (1980).
- ³⁴J. M. Bowman, J. S. Bittman, and L. B. Harding, J. Chem. Phys. **85**, 911 (1986).
- ³⁵D. Wang and J. M. Bowman, Chem. Phys. Lett. **235**, 277 (1995).
- ³⁶S. K. Gray, J. Chem. Phys. **96**, 6543 (1992).
- ³⁷R. N. Dixon, J. Chem. Soc., Faraday Trans. **88**, 2575 (1992).
- ³⁸H. J. Werner, C. Bauer, P. Rosmus, H. M. Keller, M. Stumpf, and R. Schinke, J. Chem. Phys. **102**, 3593 (1995).
- ³⁹A. Loettgers, A. Untch, H. M. Keller, R. Schinke, H. J. Werner, C. Bauer, and P. Rosmus, J. Chem. Phys. **106**, 3186 (1997).
- ⁴⁰J. S. Francisco, A. N. Goldstein, M. A. Robb, and I. H. Williams, Chem. Phys. Lett. **191**, 13 (1992).
- ⁴¹M. R. Manaa and D. R. Yarkony, J. Chem. Phys. **100**, 473 (1994).
- ⁴²B. O. Roos and K. Andersson, Chem. Phys. Lett. **245**, 215 (1995).
- ⁴³K. Andersson, P.-Å. Malmqvist, B. O. Roos, A. J. Sadlej, and K. Wolinski, J. Phys. Chem. **94**, 5483 (1990).
- ⁴⁴K. Andersson, P.-Å. Malmqvist, and B. O. Roos, J. Chem. Phys. **96**, 1218 (1992).
- ⁴⁵B. O. Roos, in *Advances in Chemical Physics: Ab Initio Methods in Quantum Chemistry-II* edited by K. P. Lawley (Wiley, Chichester, 1987), Chap. 69, p. 399.
- ⁴⁶B. O. Roos, K. Andersson, M. P. Fülscher, L. Serrano-Andrés, K. Pierloot, M. Merchán, and V. Molina, J. Mol. Struct.: THEOCHEM **388**, 257 (1996).
- ⁴⁷P. A. Malmqvist and B. O. Roos, Chem. Phys. Lett. **155**, 189 (1989).
- ⁴⁸B. O. Roos, M. P. Fülscher, Per-Åke Malmqvist, M. Merchán, and L.

- Serrano-Andrés, in *Quantum Mechanical Electronic Structure Calculations with Chemical Accuracy*, edited by S. R. Langhoff (Kluwer Academic, Dordrecht, 1995), p. 357.
- ⁴⁹P.-O. Widmark, P.-Å. Malmqvist, and B. O. Roos, *Theor. Chim. Acta* **77**, 291 (1990).
- ⁵⁰R. S. Mulliken, *J. Chem. Phys.* **23**, 1997 (1955).
- ⁵¹K. Andersson, M. P. Fülscher, G. Karlström, R. Lindh, P.-Å. Malmqvist, J. Olsen, B. O. Roos, A. J. Sadlej, M. R. A. Blomberg, P. E. M. Siegbahn, V. Kellö, J. Noga, M. Urban, and P.-O. Widmark, MOLCAS Version 3, Department of Theoretical Chemistry, Chemistry Center, University of Lund, P.O. Box 124, S-221 00 Lund, Sweden, Lund, 1994.
- ⁵²S. Califano, *Vibrational States* (Wiley, London, 1976).
- ⁵³E. B. Wilson, J. C. Decius, and P. C. Cross, *Molecular Vibrations* (McGraw-Hill, New York, 1955).
- ⁵⁴P.-Å. Malmqvist and N. Forsberg, *Chem. Phys.* (to be published).
- ⁵⁵H. Köppel, W. Domcke, and L. S. Cederbaum, *Adv. Chem. Phys.* **57**, 59 (1984).
- ⁵⁶T. Kono, M. Takayanagi, T. Nishiyama, and I. Hanazaki, *Chem. Phys. Lett.* **201**, 166 (1993).
- ⁵⁷X. M. Song and T. A. Cool, *J. Chem. Phys.* **96**, 8675 (1992).
- ⁵⁸E. Hirota, *J. Mol. Struct.* **146**, 237 (1986).
- ⁵⁹C. B. Moore and J. C. Weisshaar, *Annu. Rev. Phys. Chem.* **34**, 525 (1983).
- ⁶⁰G. K. Moortgat, W. Seiler, and P. Warneck, *J. Chem. Phys.* **78**, 1185 (1983).
- ⁶¹G. Herzberg, *Molecular Spectra and Molecular Structure. III. Electronic Spectra and Electronic Structure of Polyatomic Molecules* (Van Nostrand, New Jersey, 1966).
- ⁶²G. Herzberg, *Molecular Spectra and Molecular Structure. I. Spectra of Diatomic Molecules* (Krieger, Florida, 1989).
- ⁶³J. M. Brown, H. E. Radford, and T. J. Sears, *J. Mol. Spectrosc.* **148**, 20 (1991).
- ⁶⁴K. K. Murray, T. M. Miller, D. G. Leopold, and W. C. Lineberger, *J. Chem. Phys.* **84**, 2520 (1986).
- ⁶⁵D. A. Clabo, W. D. Allen, R. B. Remington, Y. Yamaguchi, and H. F. Schaeffer III, *Chem. Phys.* **123**, 187 (1988).
- ⁶⁶H. M. Keller, H. Floethmann, A. J. Dobbyn, R. Schinke, H. J. Werner, C. Bauer, and P. Rosmus, *J. Chem. Phys.* **105**, 4983 (1996).
- ⁶⁷S. H. Lee and I. C. Chen, *J. Chem. Phys.* **105**, 2583 (1996).
- ⁶⁸U. E. Meier, L. E. Hunziker, and D. R. Crosley, *J. Phys. Chem.* **95**, 5163 (1991).
- ⁶⁹R. S. Lowe and A. R. W. McKellar, *J. Chem. Phys.* **74**, 2686 (1981).